Control Engineering Practice 29 (2014) 299–307

Contents lists available at ScienceDirect

Control Engineering Practice

journal homepage: www.elsevier.com/locate/conengprac

Optimal energy management for an electric vehicle in eco-driving applications

Wissam Dib*, Alexandre Chasse, Philippe Moulin, Antonio Sciarretta, Gilles Corde

IFP Energies Nouvelles, 1 et 4, avenue de Bois-Préau, 92852, Rueil-Malmaison, France

ARTICLE INFO

Article history:
Received 31 May 2013
Accepted 5 January 2014
Available online 21 February 2014

Keywords:
Eco-driving
Optimal control
Electrical vehicle

ABSTRACT

This paper considers an energy management problem for an electric vehicle compliant with online requirements for 'eco-driving' application. Eco-driving techniques are discussed and formulated as an optimal control problem that consists of the minimization of the vehicle consumption over a time and distance horizon. Then, a closed-form solution of the optimal trajectories is presented. Numerical and experimental results assess the validity of the proposed eco-driving system.

1. Introduction

In recent years, environmental issues such as energy saving and reduction of CO_2 emission are emphasized. In particular, the energy consumption of automobiles accounts for a substantial amount of all transportation sectors. There are various approaches to reduce the fuel consumption of automobiles. For this purpose, high efficient powertrain and lightweight automobiles are being developed. On the other hand, the so-called "eco-driving" can also reduce the fuel consumption.

Eco-driving is now considered to be a major way of reducing the energy consumption linked to the transport of people or goods (see for example Barkenbus, 2010). Generally, the idea is that there are different ways of driving a specific journey which are not equivalent from an energy point of view. Eventually, the objective is to find the optimal one.

For personal cars, many features are proposed or will be proposed in the near future by car manufacturers. Most of the time they consist of advising the driver to change gear or to adopt a moderate velocity (Sato, Suzuki, Miya, & Iida, 2010), sometimes heuristics trajectories (Kim, Shin, Yoon, Bae, & Kim, 2011), possibly through an interface integrated in the dash boards of vehicles (Kamal, Mukai, Murate, & Kawaba, 2010).

In this context, several studies that investigate the problem of optimization of the speed trajectory of the vehicle have been reported, considering the optimal control problem of determining the velocity trajectory that minimizes the energy consumption under time constraint (Chang & Morlock, 2005; Hellstrom, Ivarsson, Aslund, & Nielsen, 2009; Saerens, Rakha, Diehl, & Van den Bulck, 2013; Stoicescu, 1995). These papers focus on applications on highway with high velocity and varying road gradients. The vehicle stops and starts that are typical of urban-like driving conditions are not taken into account.

In this paper we consider urban driving, where the vehicle trajectory is constrained by the infrastructure (road signs) and other vehicles (traffic). These constraints have a major impact on the vehicle trajectory, and therefore the formalization of the problem is different. In Dib, Serrao, and Sciarretta (2011, 2012) an approach to define and evaluate the energy efficiency of a travel for an electric car driven in such conditions has been proposed. The optimal speed trajectory was calculated using the dynamic programming algorithm (Sundstrom & Guzzella, 2009). Dynamic programming is a very powerful algorithmic paradigm (Bellman & Dreyfus, 1962), however its main disadvantage is its computational time which is relatively high.

In Petit and Sciarretta (2011) this problem has been studied and solved in closed form for an electrical car powered by a DC-type motor. The solution relies on the inversion-based methodology and several modeling assumptions. The present paper studies the problem in which an electric car powered by a PM (permanent-magnet) synchronous motor is considered. We propose a method to solve the proposed optimal control problem, similar to Petit and Sciarretta (2011) but taking into account physical limitations on the control actions and the transmission efficiency compliant with online requirements. The advantage of this solution is its computational time which is relatively small comparing with the dynamic programming algorithm, thus allowing potentially for online implementation.

The structure of the paper is as follows. In Section 2 we define the 'eco-driving' system and formulate it as an optimal control

* Corresponding author.
E-mail address: wissam.dib@ifp.fr (W. Dib).

0967-0661/$ - see front matter © 2014 Elsevier Ltd. All rights reserved.
http://dx.doi.org/10.1016/j.conengprac.2014.01.005

problem. In Section 3 we present a closed form solution of this problem defined for a specific vehicle. Then, simulation and experimental results are shown in Sections 4 and 5, respectively. Finally, we wrap up the paper with some concluding remarks in Section 6. A preliminary version of this paper has been reported in Dib, Chasse, Sciarretta, and Moulin (2012).

2. Metrics for eco-driving evaluation

2.1. Eco-driving definition

Unless a full traction control is adopted, the ultimate responsible for eco-driving is the driver. The driving action is materialized by his actions on the pedals and, consequently, a power demand is continuously established. During a road trip, the integral of this demand, E_{dem}, will not be zero because of the aerodynamic, gravity, and rolling resistance forces to overcome, as well as the energy dissipated in the friction brakes. This energy demand is fulfilled by the powertrain, and ultimately results in a consumption of the energy stored on board, E_{tank}. For a given E_{dem}, minimizing E_{tank} means optimizing the powertrain efficiency. For a given system, that can be achieved by vehicle controllers. On the other hand, minimizing E_{dem} for a given trip is the purpose of eco-driving techniques.

The driver's behavior is primarily influenced by the nature of the route to be covered and the average speed level (or, alternatively, the trip time) desired. In the case of urban trips, external factors are also particularly relevant to influence the driving style. A trip can be thus characterized as a succession of events either dictated by the driver's will or by external factors. These events are called *breakpoints* in the following. Each section of a trip between two breakpoints is called *segment*. Fig. 1 illustrates these concepts for a trip with intersections and a traffic light. Continuous traffic flow that might also constrain the driver's action is not represented in the figure.

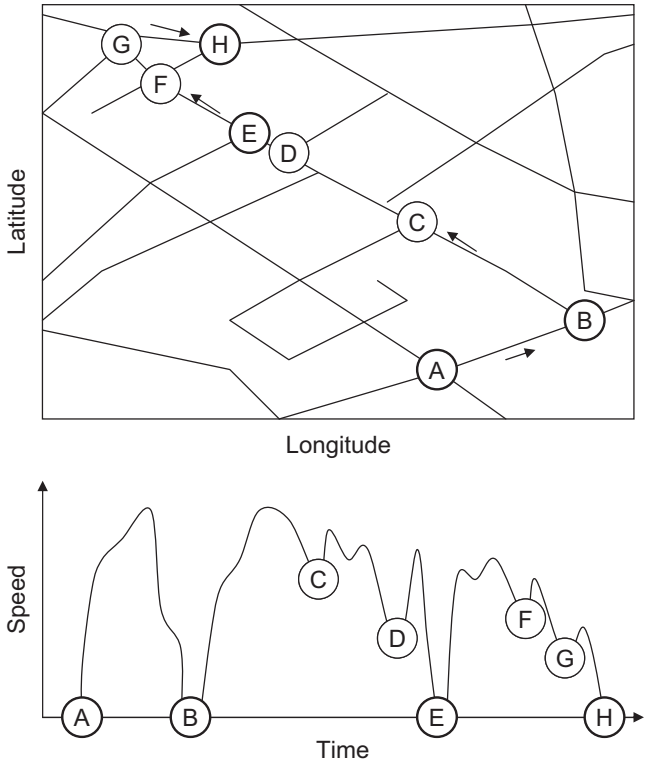

Fig. 1. Urban trip (top) and corresponding vehicle speed (bottom) with indication of the breakpoints A–H (A: start; B: intersection without priority; C, D, F, G: intersections with priority; E: traffic light; H: stop) and seven segments (A–B, B–C, etc.).

2.2. Eco-driving as an optimal control problem

Using the elements introduced in the previous section, the achievement of an eco-driving style can be formulated as an optimal control problem. This problem consists of the minimization of the vehicle energy consumption over a time and distance horizon, by acting on the driver's outputs. In the case of an electric vehicle, the energy consumption E_{tank} coincides with the battery energy consumption E_{bat} and the driver's actuators are the accelerator and brake pedal positions. Ultimately, the latter result in the motor torque τ and brake force F_{brk}. The optimization horizon is defined as a segment, i.e., the distance D between two consecutive breakpoints, while the segment duration T is given by the average speed desired. The vehicle speed v is imposed at the beginning of each segment (v_i) and at its end (v_f), that is, for each breakpoint.

In equations, find the control policy $u(t) := (\tau(t), F_{brk}(t)) \in \mathfrak{U}(t) \subset \mathbb{R}$, $t \in [0, T]$ such to

$$\min E_{bat} = \int_0^T P_{bat}(u(t), v(t), x(t))\, dt, \tag{1}$$

under the system dynamics

$$\begin{aligned} \dot{v}(t) &= f(v(t), u(t), t) - G(x(t)), \\ \dot{x}(t) &= v(t), \end{aligned} \tag{2}$$

and the following state constraints:

$$\begin{aligned} &v(0) = v_i, \quad v(T) = v_f, \\ &x(0) = 0, \quad x(T) = D, \\ &v_{min}(x(t)) < v(t) < v_{max}(x(t)), \quad x(t) \in [0, D], \end{aligned} \tag{3}$$

where $x(t)$ is the traveled distance and $v(t)$ is the speed of the vehicle, respectively. The functions $P_{bat}(\cdot)$ and $f(\cdot)$, as well as the set $\mathfrak{U}(t)$, depend on the vehicle and powertrain characteristics and will be particularized in Section 3. The parameters T, D, v_i, and v_f define the particular segment, together with the function $G(x(t))$ and the speed limits v_{min}, v_{max}. Note that $G(x(t))$ represents the gravitational force that depends on the traveled distance. For a typical trip, these parameters change for each segment. In the rest of the paper the notation T_k, D_k, etc. will be used for the kth segment.

2.3. Online implementation

The optimal control problem presented in the previous section can be solved *offline* or *online*. In the offline case, a complete trip is known in detail, with all the breakpoints and the segments completely identified by their respective parameters T_k, D_k, etc. These data are available when, e.g., an individual vehicle trip is recorded in terms of vehicle speed $v(t)$. Then, an offline optimization can be used to *assess* or qualify the recorded driving behavior by comparing its energy consumption E_{bat} with the minimum energy consumption $E_{bat,min}$ that would have been necessary to complete the trip under *the same* breakpoint constraints. An eco-driving indicator (EDI)

$$EDI = \frac{E_{bat,min}}{E_{bat}}, \tag{4}$$

can be explicitly defined in this case as proposed in Dib, Chasse, Di Domenico, et al. (2012) and it provides a quantitative and absolute basis of assessment as opposed to qualitative or arbitrary indicators.

A similar optimization can also be performed online during the vehicle trip. In this case, the future trip characteristics are not known in advance. A first scenario is an *online assessment*, where

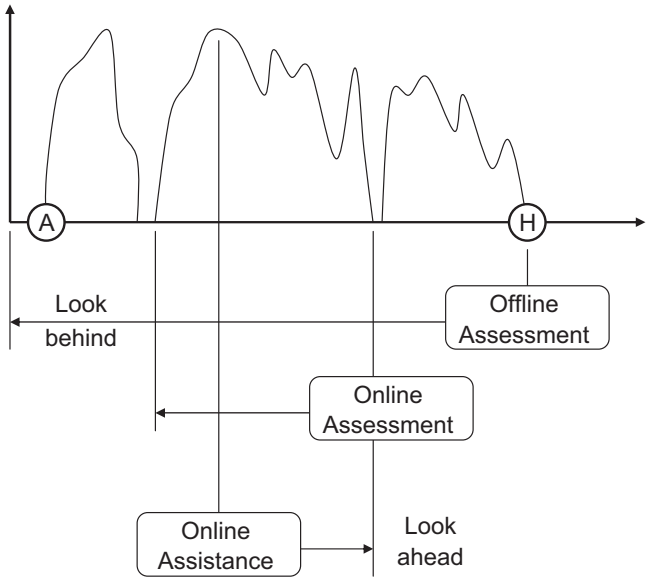

Fig. 2. Schematic of the offline assessment, online assessment, and online assistance scenarios.

the optimization is performed and the indicator is provided to the driver soon after a segment is completed. The driver is thus informed in real time about his driving style. Another scenario is the *online assistance to the driver*, where the optimization is performed continuously in time. At a time t, the optimization is performed for a segment defined by $v_i = v(t)$ and T, D, v_f as a function of the next breakpoint. The latter must thus be estimated using geo-localization, other environmental information (traffic, signals), and possibly route planning input by the driver himself. The result of the optimization is proposed to the driver and after a time step the procedure is repeated. These two online applications are illustrated in Fig. 2. In the next section we will present a closed form solution for the optimal control problem defined for a specific electric vehicle.

3. Explicit solution of the optimization problem

3.1. System modeling and optimal control problem

The vehicle is a small electric car propelled by a PM synchronous motor, connected to the rear wheels by a single-gear transmission considered with losses. A battery pack provides power to the motor through a DC/AC converter. The vehicle can be modeled as a standard drive-train, including the battery, auxiliary losses, DC/AC converter, and the electric motor (Fig. 3). The vehicle model used here is a basic longitudinal model that captures the inertial dynamics of the vehicle and the efficiency of the powertrain components, to be able to predict energy consumption. The foundation for the modeling work can be found in Guzzella and Sciarretta (2007). The motion of the vehicle can be described by Eq. (2) with

$$f(v(t),u(t),t) = \frac{\gamma\tau(t)\eta^{sign(\tau(t))}}{mR_t} - \frac{\rho_a A_f c_d}{2m}v(t)^2 - gc_r - \frac{F_{brk}(t)}{m},$$
$$G(x(t)) = g\ \sin(\alpha(x(t))), \tag{5}$$

where m is the vehicle mass (curb weight with a driver), η and γ are the efficiency and the constant ratio of the transmission respectively, ρ_a is the external air density, A_f is the vehicle frontal area, c_d is the aerodynamic drag coefficient, c_r is the rolling resistance coefficient, R_t is the wheel radius, $\alpha(x)$ is the road slope,

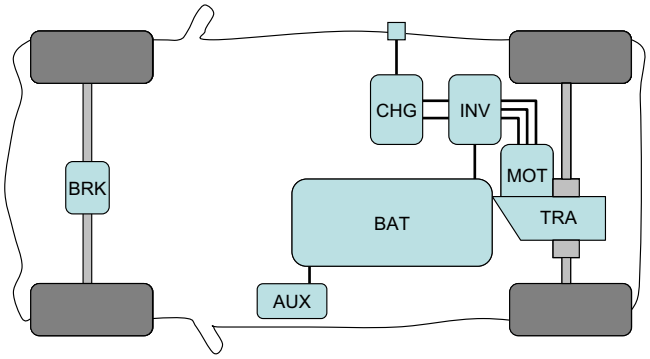

Fig. 3. Schematic of the electric vehicle configuration considered, with a battery (BAT), an external charger (CHG), auxiliary loads (AUX), a DC–AC converter (INV), a motor (MOT), a transmission (TRA), and a brake system (BRK).

and g is the acceleration of gravity. Eqs. (5) can be rewritten as

$$\dot{x} = v(t),$$
$$\dot{v} = h_1\tau(t)\eta^{sign(\tau(t))} - h_2 v(t)^2 - h_0 - w(t), \tag{6}$$

where

$$h_1 := \frac{\gamma}{mR_t}, \quad h_2 := \frac{\rho_a A_f c_d}{2m}, \quad h_0 := g\ \sin(\alpha(x(t))) + gc_r,$$

and

$$w(t) := \frac{F_{brk}(t)}{m}.$$

The power consumption can be defined as

$$P_{bat}(\tau(t), v(t)) = b_1\tau(t)v(t) + b_2\tau(t)^2, \tag{7}$$

where $b_1 := \gamma/R_t$, and b_2 is a constant to be identified (Dib, Chasse, Di Domenico, et al. 2012). The first term represents the mechanical power consumed by the vehicle while the second term represents the losses that are assumed to be function of the motor torque only (e.g., copper losses in the motor). The motor torque τ is limited by upper and lower values $\tau_M(\Omega)$ and $\tau_m(\Omega)$, respectively, where $\Omega(t) = b_1 v(t)$ is the motor speed. The brake deceleration w is limited by an upper value W.

In this case, the optimal control problem is reduced to find the control law $(\tau(t), w(t))$ such to

$$\begin{cases} \min\ \int_0^T (b_1\tau(t)v(t) + b_2\tau^2(t))\,dt, \\ \dot{v} = h_1\tau(t)\eta^{sign(\tau)} - h_2 v^2(t) - h_0 - w(t) \\ \dot{x} = v(t) \\ x(0) = 0, \quad x(T) = D \\ v(0) = v_0, \quad v(T) = v_f \\ \tau_m(v(t)) \le \tau(t) \le v_M(v(t)) \\ 0 \le w(t) \le W \end{cases} \tag{8}$$

Note that the problem formulation is similar to that in Petit and Sciarretta (2011) except for the transmission efficiency and the brake force, which are here considered in the vehicle dynamics.

3.2. Solution method

The preceding optimal control problem (8) can be solved by numerous methods. Among these are Dynamic Programming (DP), see Bellman and Dreyfus (1962) and Sundstrom and Guzzella (2009). Dynamic programming is a very powerful algorithmic paradigm in which the problem is solved by identifying a collection of subproblems and tackling them one by one, smallest first, using the answers to small problems to help figure out larger ones, until the whole lot of them is solved. Although this method is very efficient when applied to systems of low dimensions, such as the

one considered here, its main disadvantage is its computational time which is relatively high. This can reveal troublesome for higher dimensional systems and specially for online implementation. Recently, it has been applied for the same optimization problem to evaluate the energy saving potential by optimizing the speed trajectory (see Dib et al., 2011, Dib, Chasse, Di Domenico, et al. 2012). In this paper, we propose a method to solve this optimal control problem under some assumptions. Its main advantage is that it is less computationally demanding for online implementation and shows results close to those of the DP.

Consider the optimal control problem (8) and introduce the Hamiltonian

$$H = b_1\tau v + b_2\tau^2 + \lambda(h_1\eta^{sign(\tau)}\tau - h_0 - w) + \mu v, \tag{9}$$

where we neglect the aerodynamic force and define λ and μ as the two adjoint variables. The assumption of negligible air resistance is reasonable for low vehicle speeds, as it is in urban conditions, and is motivated by the major computational advantages that it allows, making the solution suitable for an online implementation. Following (Bryson, 1999), the optimal control law, in the absence of state or input constraints, is defined as

$$\{\tau^o(t), w^o(t)\} = \arg\min H(\tau, w, \lambda(t), \mu(t)), \tag{10}$$

with

$$\dot{\lambda}(t) = -\frac{\partial H}{\partial v}, \tag{11}$$

$$\dot{\mu}(t) = -\frac{\partial H}{\partial x}, \tag{12}$$

$\forall t \in [0, T]$.

These take the form

$$\begin{cases} \tau^o(t) & = \begin{cases} \tau^+(t) & \text{if } \tau^+(t) > 0, \tau^-(t) > 0 \\ 0 & \text{if } \tau^+(t) < 0, \tau^-(t) > 0 \\ \tau^-(t) & \text{if } \tau^+(t) < 0, \tau^-(t) < 0 \end{cases} \\ w^o(t) & = \begin{cases} 0 & \text{if } \lambda(t) < 0 \\ W & \text{if } \lambda(t) > 0 \end{cases} \\ \dot{\lambda}(t) & = -b_1\tau^o(t) - \mu(t) \\ \dot{\mu}(t) & = 0 \end{cases} \tag{13}$$

where $\tau^+ := -(1/2b_2)(b_1 v + h_1\eta\lambda)$, $\tau^- := -(1/2b_2)(b_1 v + (h_1\lambda/\eta))$, and W corresponds to the maximum force braking. Together with the primal equations defined in (8), they constitute a set of 4 first-order differential equations with 4 unknowns (x, v, λ, μ) and 4 end-point conditions that must be solved to eventually determine the optimal control law τ^o and w^o. Note that the presence of the term $\eta^{sign(\tau)}$ in the Hamiltonian function implies that $\tau^+(t) \neq \tau^-(t)$ and thus a discontinuity of $\tau^o(t)$, which makes the solution of this problem more complex.

3.2.1. Explicit derivation of the control law

To compute the control action $\tau^o(t)$ we assume that the maximum and minimum torque values $\tau_M(t)$ and $\tau_m(t)$ provided by the motor are constant and equal to τ_M and τ_m. This implies that the control law does not consider the flux-weakening operation range of the motor. Then two more cases can appear

- if $\tau^+(t) > \tau_M$ then $\tau^o(t) = \tau_M$,
- if $\tau^-(t) < \tau_m$ then $\tau^o(t) = \tau_m$.

Proposition 1. *Consider the vehicle model (6) where the aerodynamic friction is zero, i.e. $h_2 = 0$, and the slope is constant with the optimal control problem (8). The optimal solution (13) is well defined and given by $(\tau^o(\mu, \lambda_0), w^o(\mu, \lambda_0))$ with (μ, λ_0) the unique solution of the algebraic equations*

$$\begin{aligned} f_1(\mu, \lambda_0) &= 0, \\ f_2(\mu, \lambda_0) &= 0, \end{aligned} \tag{14}$$

with $\lambda_0 := \lambda(t)|_{t=t_0}$ and (f_1, f_2) defined by the 4 endpoint conditions.

Proof. Since the optimal motor torque $\tau^o(t)$ is discontinuous and depends on the dynamics of the vehicle and the adjoint variables, we will decompose its evolution with respect to time into six phases.

First phase: The motor torque $\tau^o(t)$ must start with a positive value to take off the vehicle. For distances long enough, we will certainly get $\tau^+(t)|_{t=t_0} > \tau_M$, therefore the first phase can be defined with the following control law:

$$\begin{aligned} \tau^o(t) &= \tau_M, \\ w^o(t) &= 0, \end{aligned} \tag{15}$$

for all $t \in [0, t_1]$ with $\tau^+(t_1) = \tau_M$.

Second phase: Once $\tau^+(t) \leq \tau_M$, a second phase will start where $\tau^o(t) = \tau^+(t)$. Therefore differentiating this equation and using the vehicle model (6), we can easily find the following:

$$\begin{aligned} \tau^o(t) &= \frac{1}{2b_2}(b_1 h_0 t + h_1\mu\eta t - h_1\lambda_0\eta - b_1 v_0), \\ w^o(t) &= 0, \end{aligned} \tag{16}$$

for all $t \in [t_1, t_2]$. The timeout of this phase t_2 is computed as $\tau^+(t_2) = 0$.

Third phase: In this case $\tau^+(t)$ becomes negative and therefore it cannot be the optimal solution. However $\tau^-(t)$ is still positive and then it is not optimal either. The optimal solution in this phase is defined as

$$\begin{aligned} \tau^o(t) &= 0, \\ w^o(t) &= 0, \end{aligned} \tag{17}$$

for all $t \in [t_2, t_3]$. The timeout of this phase is given by the condition $\tau^-(t_3) = 0$.

Fourth phase: For the next phase, the optimum is now given by the third case of (13) $\tau^o = \tau^-$. In this case

$$\begin{aligned} \tau^o(t) &= \frac{1}{2b_2}\left(\frac{h_1\mu}{\eta} + b_1 h_0\right)(t - t_3), \\ w^o(t) &= 0, \end{aligned} \tag{18}$$

for all $t \in [t_3, t_4]$. t_4 is computed such that $\tau^-(t_4) = \tau_m$.

Fifth phase: This phase is characterized again by a constant control

$$\begin{aligned} \tau^o(t) &= \tau_m, \\ w(t) &= 0, \end{aligned} \tag{19}$$

for all $t \in [t_4, t_5]$. This phase ends when $\partial H/\partial w$ change sign, i.e., when the function $\lambda(t) = 0$.

Sixth phase: Finally, the last phase corresponds

$$\begin{aligned} \tau^o(t) &= \tau_m, \\ w^o(t) &= W, \end{aligned} \tag{20}$$

for all $t \in [t_5, T]$.

Thus, assuming that all the parameters of the vehicle are known, and after some simple calculations, it is easy to show that the optimal speed $v(t)$ and distance $x(t)$ of these different phases depend only on the two unknown values (μ, λ_0) and their initial conditions $(v(0) = v_0, x(0) = 0)$. Therefore imposing the endpoint conditions $v(T) = v_f$, and $x(T) = D$, we compute the two algebraic equations $f_1(\mu, \lambda_0)$ and $f_2(\mu, \lambda_0)$. □

Proposition 2. *Consider the algebraic equations $f_1(\mu, \lambda_0)$ and $f_2(\mu, \lambda_0)$ defined above. An explicit solution of these equations can be found. That is, there exists a function $\mu(\lambda_0)$ such that $f_1(\mu(\lambda_0), \lambda_0) = 0$ and $f_2(\mu(\lambda_0), \lambda_0) = 0$.*

Proof. The equation $f_1(\mu,\lambda_0)$ which is calculated from the condition of $v(T)=v_f$ can be expressed as a first order equation in λ_0

$$f_1(\mu,\lambda_0) = -\alpha(\mu,\mu^2)\lambda_0+\beta(\mu,\mu^2,\mu^3) \tag{21}$$

where the computation of α and β is omitted here due to space limitations. Therefore, replacing $\lambda_0=\beta(\mu,\mu^2,\mu^3)/\alpha(\mu,\mu^2)$ in $f_2(\mu,\lambda_0)$ we get a tenth order equation in μ where the roots are computed by finding the eigenvalues of the corresponding companion matrix. However, only one solution has a physical interpretation.

Fig. 4 shows that different phases described above for a typical segment. Moreover, depending on the endpoint conditions and on the parameters of the segment (distance and average speed) some of these phases can disappear. Fig. 5 shows two cases where the average speed of the segment is the same while the distance is different. We can observe that the first phase disappears in the second case. This is naturally done by the construction of the solution. □

3.2.2. A simple particular case

For a sake of checking the analytical computations performed above and their forthcoming numerical implementation, it is instructive to consider the particular case where no limitations on the motor torque are considered, the mechanical brake and the transmission efficiency are neglected, i.e., $\eta=1$ and $W=0$. In this case the phases 1, 3, 5, and 6 will disappear and $\tau^+=\tau^-$. Therefore the optimal motor torque, the corresponding speed, and the instantaneous traveled distance can be expressed as

$$\begin{aligned}
\tau^o(t) &= \frac{1}{2b_2}((b_1h_0+h_1\mu)t-h_1\lambda_0-b_1v_0),\\
v(t) &= v_0+\frac{1}{4b_2}(b_1h_1h_0+h_1^2\mu)t^2-\frac{1}{2b_2}(h_1^2\lambda_0+h_1b_1v_0)t-h_0t,\\
x(t) &= v_0t+\frac{1}{12b_2}(b_1h_1h_0+h_1^2\mu)t^3-\frac{1}{4b_2}(h_1^2\lambda_0+h_1b_1v_0)t^2-\frac{h_0}{2}t^2.
\end{aligned} \tag{22}$$

The two algebraic equations are defined by

$$\begin{aligned}
f_1(\mu,\lambda_0) &= v_0+\frac{1}{4b_2}(b_1h_1h_0+h_1^2\mu)T^2-\frac{1}{2b_2}(h_1^2\lambda_0+h_1b_1v_0)T-h_0T-v_f,\\
f_2(\mu,\lambda_0) &= v_0T+\frac{1}{12b_2}(b_1h_1h_0+h_1^2\mu)T^3\\
&\quad -\frac{1}{4b_2}(h_1^2\lambda_0+h_1b_1v_0)T^2-\frac{h_0}{2}T^2-D.
\end{aligned} \tag{23}$$

Therefore, replacing the solution of the latter equations

$$\begin{aligned}
\mu &= -\frac{1}{h_1^2T^3}(24b_2D-12b_2T(v_0+v_f)+b_1h_0h_1T^3),\\
\lambda_0 &= -\frac{b_1v_0}{h_1}-(12b_2D-4b_2T(2v_0+v_f)+2b_2h_0T^2)/(h_1^2T^2)
\end{aligned} \tag{24}$$

in (22) we get a polynomial of second order for $v(t)$

$$\begin{aligned}
\tau^o(t) &= \frac{1}{h_1}\left(h_0-\frac{4v_0}{T}-\frac{2v_f}{T}+\frac{6D}{T^2}+\frac{6v_0t}{T^2}+\frac{6v_ft}{T^2}-\frac{12Dt}{T^3}\right),\\
v(t) &= v_0-\frac{4v_0t}{T}-\frac{2v_ft}{T}-\frac{6Dt^2}{T^3}+\frac{6Dt}{T^2}+\frac{3v_0t^2}{T^2}+\frac{3v_ft^2}{T^2},
\end{aligned} \tag{25}$$

which corresponds exactly to the particular solution given in Petit and Sciarretta (2011).

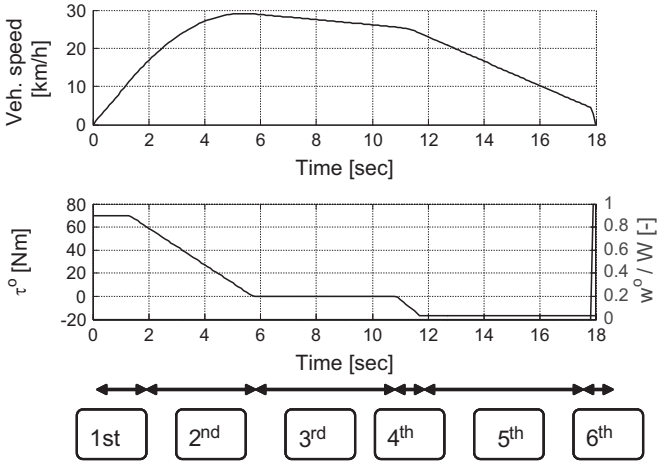

Fig. 4. Schematic of the different phases of the closed form solution.

4. Simulations

This section presents simulations of the electric vehicle described in Section 3. The parameters of the model (6) have been selected as in Dib, Chasse, Di Domenico, et al. (2012). To evaluate the performance of the proposed solution (13), we compare the energy consumption of the system using this solution and the particular case solution (25), with the one using dynamic programming. Fig. 6 shows speed trajectories of the three methods with different endpoints conditions. The simplified solution is a parabola computed from the initial speed and its final value. We also observe that the closed form solution allows higher speed values than the DP. This is mainly caused by the fact that the

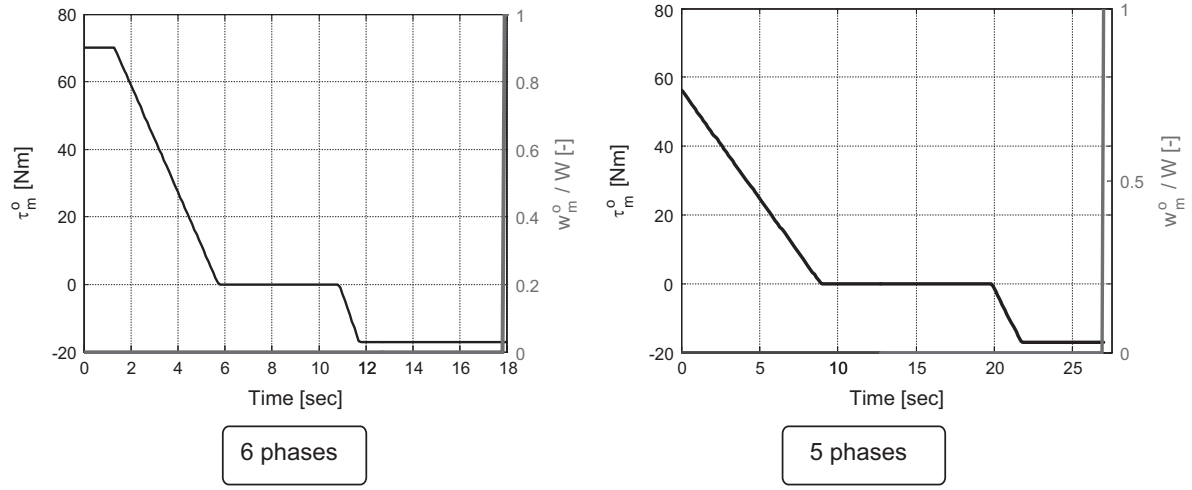

Fig. 5. Different optimal motor torque profiles.

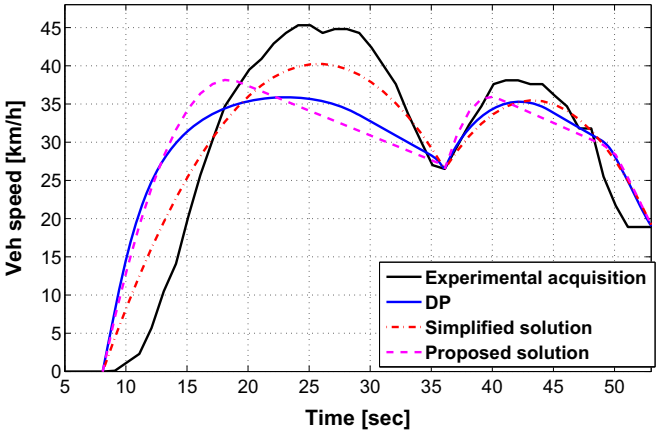

Fig. 6. Proposed solutions and the DP compared to the reference data.

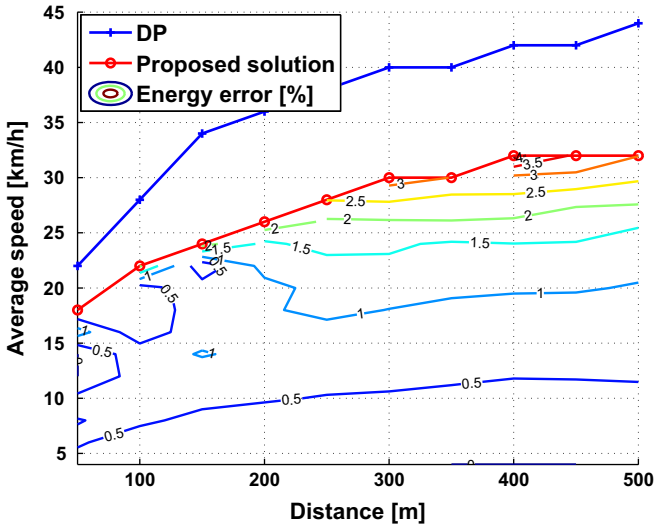

Fig. 7. Difference of the energy consumption (%): DP versus the proposed solution strategy. The average energy error is 0.98%.

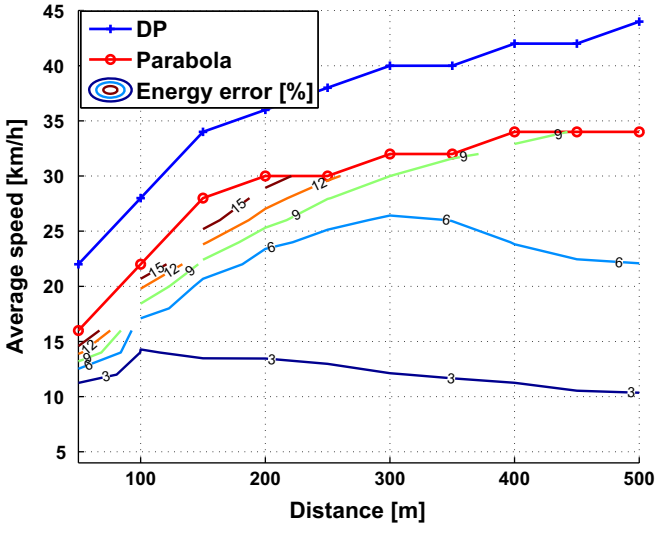

Fig. 8. Difference of the energy consumption (%): DP versus the particular case of the solution. The average energy error is 5.1%.

aerodynamic friction is being neglected in this solution. Figs. 7 and 8 show the difference in the energy consumption between the three methods as the operating range. We observe that the DP has the

Table 1
Peugeot iOn datasheet.

Performance		
Maximum speed	130 km/h	
Range	120 to 130 km	
Acceleration from 0 to 100 km/h	15.9 s	
Electrical components	Type	Power
Motor	PMSM	50 kW /67 hp
Battery	Li-ion	16 kW h
Curb weight (including driver)	1190 kg	

Fig. 9. Experimental illustration: capture of the screen 'driver-assistance' system. It shows the measured speed of the vehicle with the optimal trajectory, and the eco-driving score.

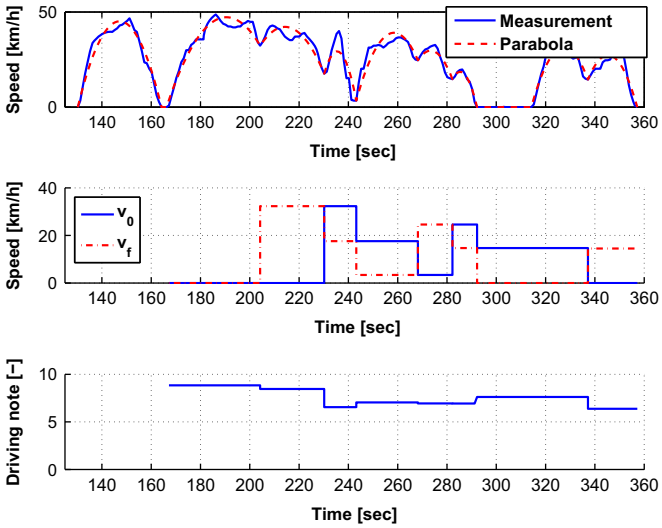

Fig. 10. Experimental illustration: description of the online assessment computation.

largest operating range. This is because the proposed solution does not treat the flux weakening operation range of the motor and considers the limitations of the control action as constant values.

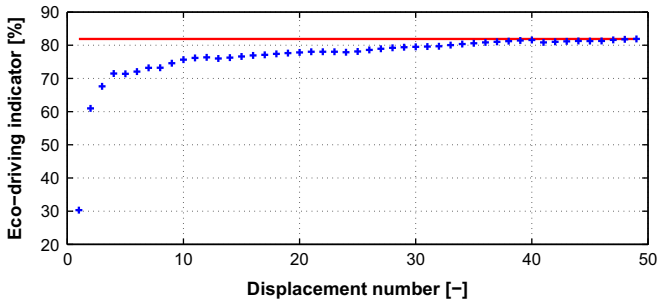

Fig. 11. Experimental illustration: evolution of the eco-driving indicator (efficiency in %) for a driver using the eco-driving system.

Moreover, the energy consumption of the system using (13) is closer to DP than the one using (25). As a conclusion, the general solution is more effective than the particular case in terms of saving energy. However, the particular solution is easier to implement. Note that to calculate the energy consumption of the system, the overall model (5) of the system is used in a backward mode where for a given speed profile we compute the power consumed.

5. Experimental illustration

5.1. Online assessment integration

This section presents experimental results of an "online assessment" integration in an electrical vehicle. The characteristics of the vehicle used (Peugeot iOn) are given in Table 1.

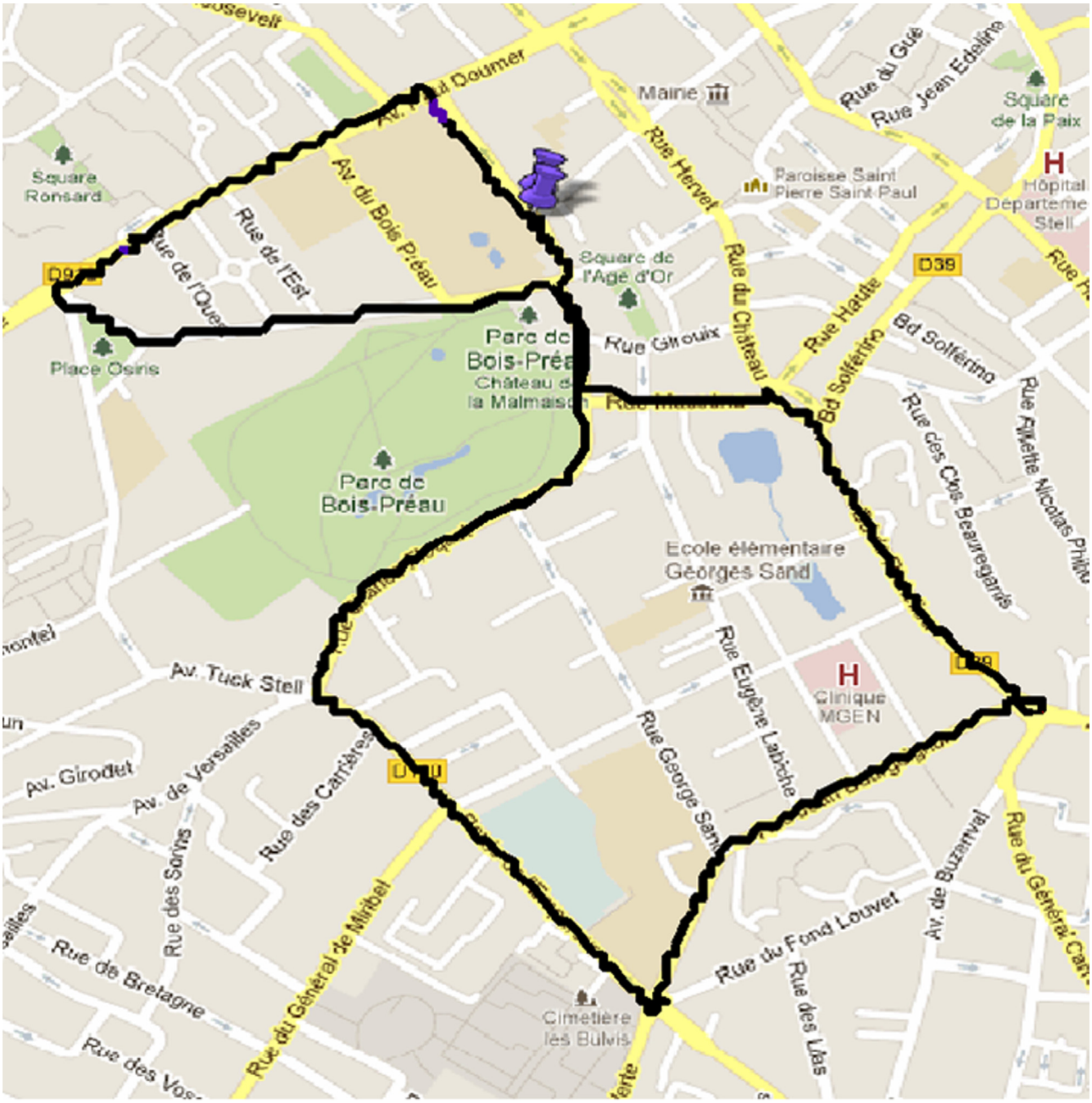

Fig. 12. Experimental test campaign: route driven by the different drivers.

The purpose of this system is to evaluate the driving of the user in terms of energy consumption with the eco-driving indicator. Therefore at each breakpoint, the human–machine interface of this system, as shown in Fig. 9, shows the speed trajectory of the vehicle with the optimal one, and compares the corresponding energies.

This first version integrates the online computation of the particular solution explained above (generic parabola). Its computation time is low and acceptable by the calculator integrated in the vehicle for the client services. Fig. 10 shows the vehicle speed evolution with the computation of two of the inputs of the optimal trajectory (initial and final speed) and the outputs of the online assessment, i.e., the optimal speed profile and the driving score. The eco-driving score (EDS) is defined as a function of the EDI,

$$EDS = 10\left(2 - \frac{1}{EDI}\right) \tag{26}$$

The best score is obtained when the electric energy consumption corresponds to the optimal one and the score vanishes when the consumed energy doubles the optimal one. Therefore, this system will help the driver to change his behavior in order to reduce the electrical energy consumption and thus increase his driving efficiency and the vehicle range. Fig. 11 shows the evolution of the eco-driving indicator for a specific client on a trip of 10 km. We can observe that the driver takes account of the online driving assessment, thus changing his behavior and reducing the electrical energy consumption of the vehicle.

5.2. Experimental test campaign

This section presents the results of an experimental test campaign aiming at the evaluation of the presented eco-driving system on twenty different drivers. The route is shown in Fig. 12. It consists in a total distance of 5 km in an urban environment with slopes, stops, and many traffic lights. Each participant drives the same route twice. The first round is done without the proposed eco-driving system that is activated only during the second round. The purpose is to evaluate the gain in terms of energy efficiency of the eco-driving system with diverse driver profiles. We recall that the optimal solution used for the test is the particular solution defined in Section 3.2.2. Fig. 13 shows the percentage of displacements during the whole route as a function of the EDI for the first and second rounds. We can observe that, with the use of the eco-driving system, more segments present higher indicators. This implies that the drivers enhanced the efficiency of their driving behavior during the second round.

Table 2 presents the evolution of the energy consumption, speed, EDI and optimal energy between the first and second rounds, averaged for all the participants. We can observe that when the proposed eco-driving system is used, the EDI is augmented by 6.1%, the optimal energy is decreased by 8.9% and the average speed is decreased by 2%. As a consequence, the average energy consumption is decreased by 14.1%. Note that decreasing the average trip speed and the optimal energy are not the main purpose of the proposed system. Indeed the aforementioned optimal solution should maintain the same time trip by construction. It seems that the driver behavior is changed by the eco-driving system, resulting in more anticipation and smoother trajectories. Of course these indirect effects are not an issue because they are beneficial in terms of energy consumption.

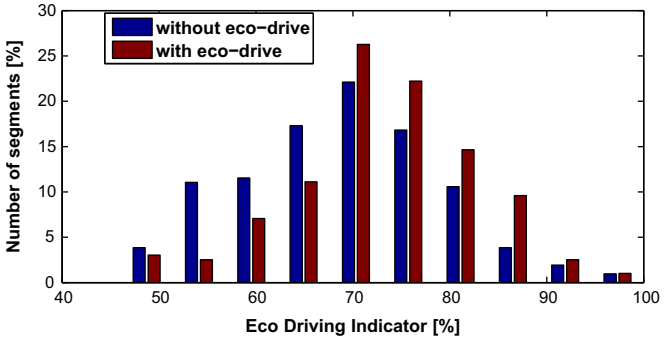

Fig. 13. Experimental test campaign: percentage of number of segments as a function of the indicator.

Table 2
Experimental test campaign, comparison between first (without eco-driving) and second round (with eco-driving): average energy consumed, average speed, average indicator and average optimal energy.

	Baseline	Eco-driving
Average energy consumption (W h/km)	115.6	99.3
Average EDI (%)	69.2	73.4
Average speed (km/h)	27.6	26.9
Average optimal energy (W h/km)	80.1	72.9

6. Conclusion and future work

The potentiality for saving energy by optimizing the speed trajectory has been discussed. It has been shown that the problem of finding an optimal speed trajectory is equivalent to the problem of solving a system of two algebraic equations. Furthermore an optimal control law whose performances in terms of energy saving are very close to those of the DP has been proposed. To the best of our knowledge, no equivalent result is available in the literature at this level of generality. The particular case of this solution has been implemented on board of an electrical vehicle for eco-driving purpose. Numerical and experimental results assess the validity of the proposed eco-driving system. The next steps of this work are the implementation of the general solution on board and to provide an online assistance to the driver. This will be possible by using other environmental information such as the state of the traffic lights.

Acknowledgments

This work was done within the project VME (Ville, Mobilité, Energie) with the collaboration of VULOG (http://www.vulog.fr) and the LE2I Laboratory UMR-CNRS (http://le2i.cnrs.fr). It has been partially supported by the French Environment and Energy Management Agency (ADEME).

References

Barkenbus, J. (2010). Eco-Driving: *An overlooked climate change initiative. Energy Policy*, 762–769.
Bellman, R., & Dreyfus, S. (1962). *Applied dynamic programming*. Princeton, NJ: Princeton University Press.
Bryson, A. E. (1999). *Dynamic optimization*. Chicago: Addison Wesley.
Chang, D., & Morlock, E. (2005). Vehicle speed profiles to minimize work and fuel consumption. *Journal of Transportation Engineering*(March), 131–173.
Dib, W., Chasse, A., Di Domenico, D., Moulin, P., & Sciarretta, A. (2012). Evaluation of the energy efficiency of a fleet of electric vehicle for eco-driving application. In *Oil & gas science and technology – Revue de IFP Energies nouvelles*.
Dib, W., Chasse, A., Sciarretta, A., & Moulin, P. (2012). Optimal energy management compliant with online requirements for an electric vehicle in eco-driving applications. In *IFAC workshop on engine and powertrain control, simulation and modeling*.
Dib, W., Serrao, L., & Sciarretta, A. (2011). Optimal control to minimize trip time and energy consumption in electric vehicles. In *7th IEEE vehicle power and propulsion conference*, September.

Guzzella, L., & Sciarretta, A. (2007). *Vehicle propulsion systems – introduction to modeling and optimization*. Berlin: Springer Verlag.

Hellstrom, E., Ivarsson, M., Aslund, J., & Nielsen, L. (2009). Lookahead control for heavy trucks to minimize trip time and fuel consumption. *Control Engineering Practice*, *17*, 245–254.

Kamal, M. A. S., Mukai, M., Murate, J., & Kawaba, T. (2010). On board eco-driving system for varying road-traffic environment using model predictive control. In *Proceedings of the IEEE conference on control applications*.

Kim, S.-Y., Shin, D.-J., Yoon, H.-J., Bae, H.-C., & Kim, D.-S. (2011). Development of eco driving guide system. In *SAE asia pacific automotive engineering conference*, 2011-28-0034.

Petit, N., & Sciarretta, A. (2011). Optimal drive of electric vehicles using an inversion-based trajectory generation approach. In *IFAC World congress*.

Saerens, B., Rakha, H. A., Diehl, M., & Van den Bulck, E. (2013). A methodology for assessing eco-cruise control for passenger vehicles. *Transportation Research Part D*, *19*, 20–27.

Sato, S., Suzuki, H., Miya, M., Iida, N. (2010). Analysis of the effect of eco-driving with early shift-up on real-world emission. In *Society of automotive engineering*.

Stoicescu, A. P. (1995). On fuel-optimal velocity control of a motor vehicle. *International Journal of Vehicle Design*, *17*, 229–256.

Sundstrom, O., & Guzzella, L. (2009). A generic dynamic & programming Matlab function. *IEEE Control Applications Intelligent Control*, 1625–1630.